

## Controlled growth of Zn-polar ZnO film on MgAl<sub>2</sub>O<sub>4</sub> (1 1 1) substrate using MgO buffer layer

This article has been downloaded from IOPscience. Please scroll down to see the full text article.

2010 J. Phys. D: Appl. Phys. 43 085301

(<http://iopscience.iop.org/0022-3727/43/8/085301>)

[The Table of Contents](#) and [more related content](#) is available

Download details:

IP Address: 159.226.36.135

The article was downloaded on 11/02/2010 at 06:12

Please note that [terms and conditions apply](#).

# Controlled growth of Zn-polar ZnO film on MgAl<sub>2</sub>O<sub>4</sub> (1 1 1) substrate using MgO buffer layer

Zhaoquan Zeng<sup>1,5</sup>, Yuzi Liu<sup>1</sup>, Hongtao Yuan<sup>1</sup>, Zengxia Mei<sup>1</sup>, Xiaolong Du<sup>1,6</sup>, Jinfeng Jia<sup>2</sup>, Qikun Xue<sup>1,2,6</sup>, Ze Zhang<sup>3</sup> and Gregory J Salamo<sup>4</sup>

<sup>1</sup> Beijing National Laboratory for Condensed Matter Physics, Institute of Physics, Chinese Academy of Sciences, Beijing 100190, People's Republic of China

<sup>2</sup> Department of Physics, Tsinghua University, Beijing 100084, People's Republic of China

<sup>3</sup> Institute of Microstructure and Property of Advanced Materials, Beijing University of Technology, Beijing 100022, People's Republic of China

<sup>4</sup> Department of Physics, University of Arkansas, Fayetteville, AR 72701, USA

E-mail: [xldu@aphy.iphy.ac.cn](mailto:xldu@aphy.iphy.ac.cn) and [qkxue@mail.tsinghua.edu.cn](mailto:qkxue@mail.tsinghua.edu.cn)

Received 2 December 2009, in final form 12 January 2010

Published 11 February 2010

Online at [stacks.iop.org/JPhysD/43/085301](http://stacks.iop.org/JPhysD/43/085301)

## Abstract

A pure rocksalt MgO buffer layer was used to modify the surface structure of MgAl<sub>2</sub>O<sub>4</sub> (1 1 1) substrates to achieve growth of a Zn-polar ZnO film by radio frequency plasma-assisted molecular beam epitaxy. It is found that this pure rocksalt MgO buffer layer plays a crucial role in 30° rotation domain elimination, surface morphology improvement and Zn-polarity control of the ZnO film, as demonstrated by *in situ* reflection high-energy electron diffraction and *ex situ* transmission electron microscopy. Atomic force microscopy observation also illustrates a smooth surface for the ZnO film.

Owing to the large free exciton binding energy of 60 meV, ZnO, as a wide-band-gap oxide semiconductor, has enormous potential applications in short-wavelength optoelectronic devices, particularly in low-threshold excitonic laser diodes (LDs) [1]. For these applications, high-quality ZnO films with single polarity are essential since polarity is a key factor that affects their growth modes, electronic properties and p-type doping efficiency [2–4]. By far, polarity manipulation of hetero-epitaxial ZnO films remains a great challenge in spite of many efforts. Sapphire (0 0 0 1) substrates have been extensively used for the growth of ZnO films. However, the epitaxial orientation with a well-known 30° in-plane rotation between ZnO (0 0 0 1) and sapphire (0 0 0 1) makes it very difficult to obtain high-quality cavity mirrors for ZnO LDs by cleaving the sapphire substrate [5]. As an alternative substrate, MgAl<sub>2</sub>O<sub>4</sub> (1 1 1) has also been adopted for epitaxy of high-quality ZnO films. By using Mg modification of an O-terminated MgAl<sub>2</sub>O<sub>4</sub> (1 1 1) surface, 30° rotation domains

and inversion domains were eliminated, and O-polar ZnO films with an overlapped in-plane orientation have been achieved in our previous work [6]. Nonetheless, growth of Zn-polar ZnO film on this substrate, however, has not been reported. In this paper, we focus on the controlled growth of Zn-polar ZnO films with an epitaxial orientation without in-plane rotation by using a pure rocksalt MgO (RS-MgO) buffer layer.

The MgO buffer layer technique has already been used to grow ZnO on sapphire (0 0 0 1) substrates [7–10] which drastically improves the quality of ZnO films. In these works, MgO was not only used to reduce the big lattice mismatch between ZnO and the substrate, but also to control the polarity of the ZnO films, i.e. an ultra-thin (less than 3 nm) wurtzite MgO (WZ-MgO) buffer results in O-polar ZnO, whereas a RS-MgO buffer results in Zn-polar ZnO. It should be noted that in many cases, the buffer contains both WZ-MgO and RS-MgO. Therefore, a disordered interface is often observed. In this work, we obtained pure RS-MgO by optimizing the growth conditions of MgO on the MgAl<sub>2</sub>O<sub>4</sub> (1 1 1) surface, which resulted in a single Zn-polar ZnO film with a sharp interface. We also found that the strain in ZnO caused by the

<sup>5</sup> Present address: Department of Physics, University of Arkansas, Fayetteville, AR 72701, USA.

<sup>6</sup> Authors to whom any correspondence should be addressed.

lattice mismatch was relaxed promptly by the double-buffer growth process.

A radio frequency (rf) plasma-assisted molecular beam epitaxy (MBE) system (OmniVac) was used to grow ZnO films on  $\text{MgAl}_2\text{O}_4$  (1 1 1) substrates. The substrates were degreased in trichloroethylene and acetone and rinsed with de-ionized water before introduced into the load lock. In the growth chamber, they were thermally cleaned at 780 °C for 20 min, and then pretreated by oxygen radicals for 30 min with a rf power of 400 W and an oxygen flux of 2.0 SCCM (SCCM denotes cubic centimetres per minute at STP) at a substrate temperature of 600 °C. After the above-mentioned high temperature degassing and pretreatment by oxygen radicals, two samples under different growth conditions for MgO buffer layer were studied. For sample A, a more than 3 nm thick MgO buffer layer was directly deposited at an initial growth rate lower than 0.02 nm min<sup>-1</sup>. Then a conventional two-step growth of ZnO film, i.e. a low temperature buffer layer growth at 380 °C and a high temperature growth at 650 °C, was performed. Inversion domains were observed in the ZnO film. For sample B, a MgO buffer layer was deposited at a higher growth rate of 1 nm min<sup>-1</sup>, then the same two-step growth of ZnO film as sample A was used. No inversion domains were observed in sample B, and zinc polarity was confirmed with TEM techniques, which will be discussed later. During the MgO buffer layer growth, the oxygen rf plasma source was kept at 300 W with an oxygen flow rate of 1.5 SCCM, and the growth rate was controlled by a Mg beam flux. For all ZnO film growth processes, the Zn beam flux was fixed at  $1.2 \times 10^{-6}$  Torr. However, different rf powers and oxygen flow rates were adopted for different growth steps, i.e. 230 W and 1.3 SCCM for the buffer layer, and 400 W and 2.0 SCCM for the epilayer. The duration of epilayer growth was 3 h.

Figures 1(a) and (b) show the reflection high-energy electron diffraction (RHEED) patterns of sample A before and after MgO growth, respectively. Figure 1(a) is taken from the substrate surface right after the pretreatment by oxygen radicals. The sharp streaky RHEED pattern indicates a clean and flat surface after thermal cleaning and pretreatment by oxygen radicals. When MgO growth begins, the sharp streaky RHEED pattern disappears gradually, and a dim and streaky pattern appears. As MgO grows, the streaks become more and more sharp (figure 1(b)), indicating a two-dimensional (2D) growth mode. Further growth of MgO leads to a diffuse spotty pattern (figure 1(c)), which indicates the transition of growth modes from 2D to three-dimensional (3D). As the thickness of MgO increases, another set of symmetrical spots appears and mixes with the above diffuse spotty pattern (figure 1(d)), which has proved to be the mixed phase of WZ-MgO and RS-MgO with 60° or 180° twin crystals in virtue of the kinematical selected area diffraction pattern (SADP) simulation by Zuo and Mabon [11], consistent with the subsequent high-resolution transmission electron microscopy (HRTEM) observations. Figure 1(e) shows the RHEED pattern of MgO after 750 °C annealing for 15 min. It is clear that the arrangement of diffraction spots in figure 1(e) is unchanged compared with that in figure 1(d), indicating that the mixed phase of WZ-MgO and RS-MgO with 60° or 180° twin crystals is stable under the

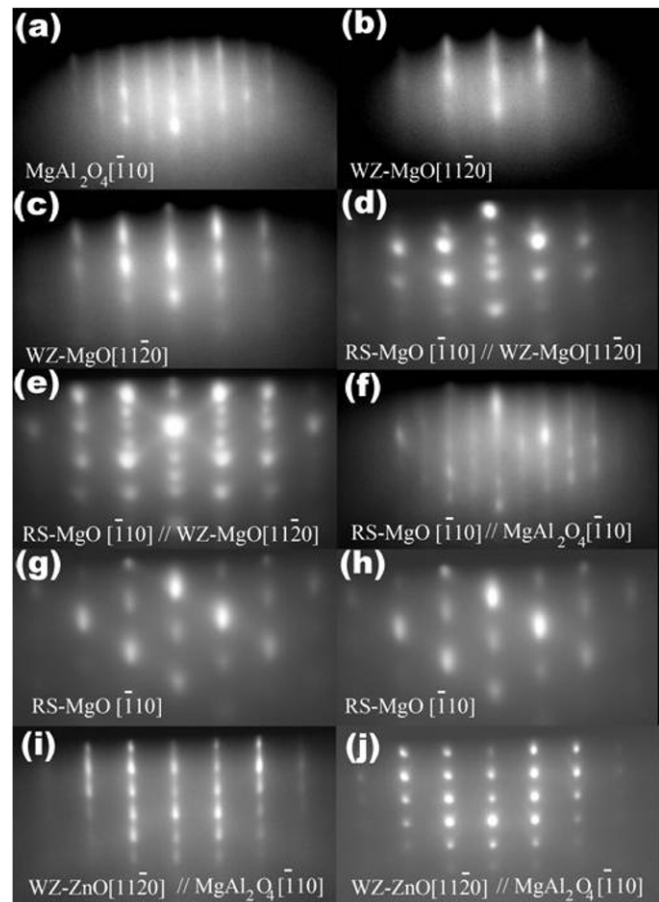


**Figure 1.** RHEED patterns taken from (a) the clean  $\text{MgAl}_2\text{O}_4$  (1 1 1) substrate, (b) during 2D growth of MgO in sample A, (c) during 2D–3D growth transition of MgO in sample A, (d) the mixed phase of MgO in sample A, (e) the annealed mixed phase of MgO in sample A, (f) at the beginning of MgO buffer layer in sample B, (g) at the end of MgO buffer layer in sample B, (h) the annealed MgO in sample B, (i) the annealed ZnO buffer layer in sample B and (j) the ZnO epilayer in sample B.

above variable temperature conditions. Finally, the ZnO film was grown on this MgO buffer layer. Although the ZnO film has the epitaxial orientation in which the surface lattice of ZnO (0 0 0 1) overlaps that of the substrate, inversion domains were observed in sample A, which was demonstrated by a convergent beam electron diffraction (CBED) experiment [12] (not shown here).

On the other hand, no inversion domains were formed in sample B. The same sharp streaky pattern as that from sample A (figure 1(a)) is observed after oxygen plasma pretreatment (not shown here). However, this pattern becomes dim immediately and a set of nonsymmetrical spots is superimposed on it when MgO growth begins on this O-terminated surface (figure 1(f)). As MgO grows, this set of spots is further enhanced and remains till the end (figure 1(g)). It is clear that this set of spots corresponds to pure RS-MgO without twin crystals in virtue of the kinematical SADP simulation [11]. Figure 1(h) is the RHEED pattern of MgO after 750 °C annealing for 15 min, and no change occurs compared with figure 1(g), indicating that pure RS-MgO without twin crystals is also stable like sample A. When the ZnO buffer

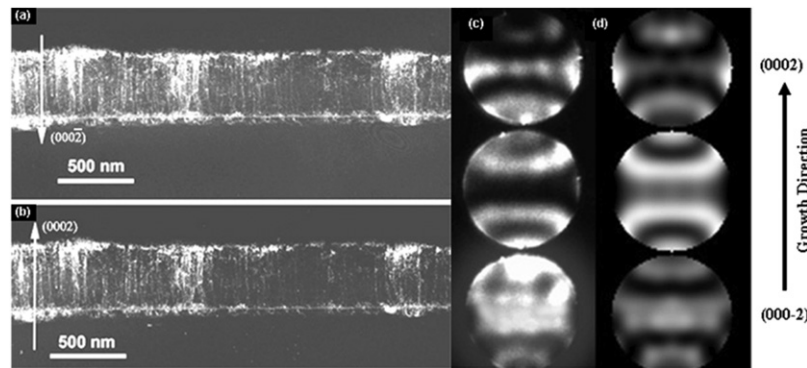


**Figure 2.** Cross-sectional TEM images showing uniform Zn-polarity ZnO films formed in sample B: (a) weak-beam dark-field cross-sectional TEM image along  $g = (000 - 2)$ ; (b) weak beam dark-field cross-sectional TEM image along  $g = (000 2)$ ; (c) experimental CBED pattern; (d) simulation CBED pattern with Zn-polarity and a thickness of 140 nm.

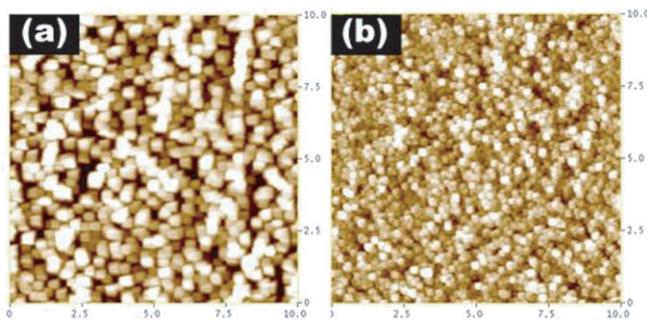


**Figure 3.** AFM images taken from as-grown ZnO films of samples A (a) and B (b). Image size:  $10 \times 10 \mu\text{m}^2$ .

(This figure is in colour only in the electronic version)

layer is deposited on this pure RS-MgO, one set of spotty pattern is observed (figure 1(i)), indicating the formation of a single-domain ZnO with an in-plane epitaxial relationship of  $\text{ZnO}[11\bar{2}0]/\text{MgAl}_2\text{O}_4[\bar{1}10]$ . Distinct from O-polar ZnO film [6], the spotty patterns exist during the entire buffer layer and epilayer growth, indicating small lattice mismatch and typical 3D growth mode. After epilayer growth for 3 h, a set of spotty patterns with clear Kikuchi lines was observed (figure 1(j)), suggesting good crystallinity. CBED experiment [12] indicated that no inversion domains were observed and a Zn-polar ZnO film was formed in sample B, illustrated by figure 2.

CBED experiment result is also consistent with the contrast of growth rate and surface morphology of samples A and B. Derived from the film thickness characterized by a Dektak 8 stylus profiler (DI, Veeco Metrology Group), the growth rate of samples A and B is about 1.2 and 1.5 times more than that of a typical O-polar ZnO film under the same growth conditions [6], respectively, consistent with the previous results [10] that the growth rate of the Zn-polar ZnO film is 1.5 times more than that of the O-polar film. The difference in growth rate and growth mode results in a distinct surface morphology, as shown in figure 3 by atomic force microscopy (AFM). On an area of  $10 \times 10 \mu\text{m}^2$ , the root-mean-square (RMS) roughnesses are 35.734 nm and 5.627 nm for samples A and B, respectively. Both growth rate and AFM characterization further confirm the polarity determination result of samples A and B by CBED experiment.

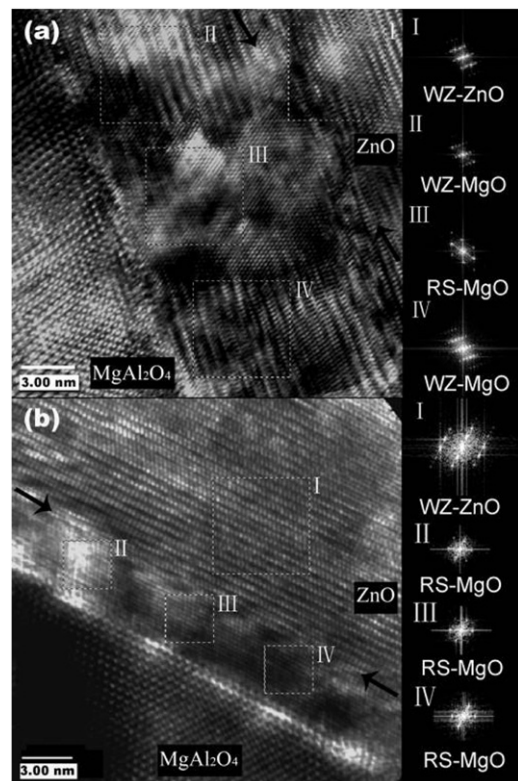


**Figure 4.** Cross-sectional HRTEM images of ZnO/MgO/MgAl<sub>2</sub>O<sub>4</sub> heterostructures in samples A (a) and B (b) with the zone axis of ZnO[11 $\bar{2}$ 0]. The right rows show the corresponding FFT images of the selected regions in samples A and B.

To further clarify the role of MgO in the polarity selection of ZnO film, a HRTEM experiment was performed near the interface along ZnO[11 $\bar{2}$ 0]direction. Figure 4(a) gives the HRTEM images of sample A. It is obvious that the interface is disordered and two kinds of MgO were formed between the ZnO film and the substrate by fast Fourier transform (FFT) analysis: one is WZ-MgO in regions II and IV, and the other is RS-MgO without twin crystals in region III. Figure 4(b) gives the HRTEM images of sample B. It can be seen that pure RS-MgO without twin crystals was formed at the interface by FFT analysis, resulting in a very sharp interface in the ZnO/MgO/MgAl<sub>2</sub>O<sub>4</sub> sandwich structure. Based on these observations, we can conclude that a low growth rate conduces

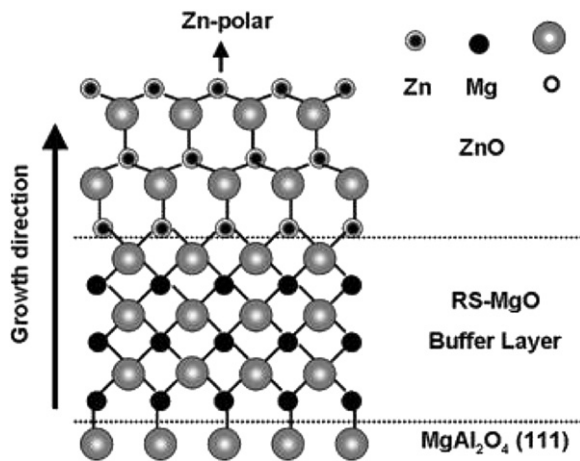


**Figure 5.** Atomic model proposed for the interface structures between  $\text{MgAl}_2\text{O}_4$  (1 1 1) substrate and ZnO film in sample B.

to the nucleation of WZ-MgO, whereas a high growth rate to that of RS-MgO on  $\text{MgAl}_2\text{O}_4$  (1 1 1) substrates.

Obviously, the pure RS-MgO plays a crucial role in the growth of single-domain Zn-polar ZnO film on  $\text{MgAl}_2\text{O}_4$  (1 1 1) substrates. For sample A, WZ-MgO, together with RS-MgO with  $60^\circ$  or  $180^\circ$  twin crystals, nucleated at the interface and grew up, although WZ-MgO was the primary one at the beginning, resulting in the disordered interface and the formation of inversion domains in ZnO film. For sample B, a pure RS-MgO without twin crystals was formed at a high growth rate, resulting in the growth of Zn-polar film. In this epitaxy system, the dependence of ZnO film polarity on the structure of MgO is very similar to that of the ZnO/MgO/ $\text{Al}_2\text{O}_3$  (0 0 0 1) system [7]. It should be noted that there are two differences in this system: one is that WZ-MgO does not have a critical thickness from wurzite structure to rocksalt structure, and the other is that pure RS-MgO can be formed at the interface. Although many studies have been done on RS-MgO (1 1 1) surfaces [13–18], the mechanism of Zn-polarity selection for ZnO on this surface is still not clear. Figure 5 only shows a tentative atomic model of the interface between the substrate and the ZnO film based on our observations. The stable mechanisms of WZ-MgO and RS-MgO on  $\text{MgAl}_2\text{O}_4$  (1 1 1), as well as their effects on the polarity selection of ZnO film, have been studied systematically and will be published elsewhere.

In summary, by the use of a pure RS-MgO buffer layer, a Zn-polar ZnO epitaxial film with a sharp interface

and overlapped in-plane orientation has been obtained on a  $\text{MgAl}_2\text{O}_4$  (1 1 1) substrate, and an atomic model is proposed to explain the mechanism of Zn-polarity selection for the ZnO film. Such smooth films should be promising for preparing high performance quantum structures.

## Acknowledgment

This work is financially supported by the National Science Foundation of China (under Grant No 50532090), the Ministry of Science and Technology of China (under Grant Nos 2007CB936203 and 2009CB929400) and the Chinese Academy of Sciences.

## References

- [1] Look D C 2001 *Mater. Sci. Eng. B* **80** 383
- [2] Li L K, Jurkovic M J, Wang W I, Van Hove J M and Chow P P 2000 *Appl. Phys. Lett.* **76** 1740
- [3] Sumiya M, Yoshimura K, Ohtsuka K and Fuke S 2000 *Appl. Phys. Lett.* **76** 2098
- [4] Look D C, Reynolds D C, Litton C W, Jones R L, Eason D B and Cantwell G 2002 *Appl. Phys. Lett.* **81** 1830
- [5] Chen Y F, Hong S K, Ko H J, Nakajima M, Yao T and Segawa Y 2000 *Appl. Phys. Lett.* **76** 245
- [6] Zeng Z Q, Liu Y Z, Yuan H T, Mei Z X, Du X L, Jia J F, Xue Q K and Zhang Z 2007 *Appl. Phys. Lett.* **90** 081911
- [7] Kato H, Miyamoto K, Sano M and Yao T 2004 *Appl. Phys. Lett.* **84** 4562
- [8] Chen Y F, Ko H J, Hong S K and Yao T 2000 *Appl. Phys. Lett.* **76** 559
- [9] Ko H J, Yao T, Chen Y F and Hong S K 2002 *J. Appl. Phys.* **92** 4354
- [10] Minegishi T, Yoo J, Suzuki H, Vashaei Z, Inaba K, Shim K and Takafumi Y 2005 *J. Vac. Sci. Technol. B* **23** 1286
- [11] Zuo J M and Mabon J C 2004 *Web-based Electron Microscopy Application Software: Web-EMAPS, Microsc. Microanal. (Suppl 2)* **10** URL: <http://emaps.mrl.uiuc.edu/>
- [12] Romano L T, Northrup J E and OKeefe M A 1996 *Appl. Phys. Lett.* **69** 2394
- [13] Kiguchi M, Entani S, Saiki K, Goto T and Koma A 2003 *Phys. Rev. B* **68** 115402
- [14] Lazarov V K, Weinert M, Chambers S A and Gajdardziska-Josifovska M 2005 *Phys. Rev. B* **72** 195401
- [15] Wander A, Bush I J and Harrison N M 2003 *Phys. Rev. B* **68** 233405
- [16] Goniakowski J, Noguera C and Giordano L 2004 *Phys. Rev. Lett.* **93** 215702
- [17] Grigorov I L, Fitzsimmons M R, Siu I L and Walker J C 1999 *Phys. Rev. Lett.* **82** 5309
- [18] Lazarov V K, Zimmerman J, Cheung S H, Li L, Weinert M and Gajdardziska-Josifovska M 2005 *Phys. Rev. Lett.* **94** 216101